Theoretical study on the excited and ionized states of titanium tetrachloride

Hiroshi Nakatsuji and Masahiro Ehara
Department of Synthetic Chemistry, Faculty of Engineering, Kyoto University, Kyoto 606, Japan and Institute for Fundamental Chemistry, Nishi-Hiraki-cho, Kyoto 606, Japan

Michael H. Palmer
Department of Chemistry, University of Edinburgh, EH9 3JJ, Scotland

Martyn F. Guest
SERC Daresbury Laboratory, Warrington, WA4 4AD, England

(Received 6 March 1992; accepted 4 May 1992)

The excitation and ionization spectra of $TiCl_4$ have been studied theoretically by the symmetry adapted cluster (SAC)/SAC-CI and multireference CI (MRD-CI) methods. The calculated spectra show good agreement with the observed spectra. The present results indicate several new assignments for the excitation spectrum. The peaks below 8.0 eV are assigned to valence excitations and those at 9.35 and 10.04 eV are assigned to Rydberg-type excitations within chlorine ligands. The ordering of the ionized states in the outer valence region is $(1t_1)^{-1} < (3t_2)^{-1} < (1e)^{-1} < (2t_2)^{-1} < (2a_1)^{-1}$, which supports the result of earlier Green's function calculations.

I. INTRODUCTION

Titanium tetrachloride is both a fundamental molecule and typical of the tetrahedral compounds of transition metals. Furthermore, it is important in both organic and inorganic chemistry as a Lewis acid. For example, $TiCl_4$ plays an important role in polymerization of alkenes by Ziegler–Natta catalysis.

A number of experimental studies have been reported to investigate the electronic structure of this important molecule. Details of the electronic excitation spectrum have been observed over a wide energy range up to the vuv region.[1–5] A schematic diagram of the spectrum is shown in Fig. 1; there are five main bands in the region from 4 to 10 eV, of which the three at highest energy are the strongest.

The uv photoionization spectrum of $TiCl_4$ has also been investigated intensively; the He(I) and He(II) photoelectron spectra observed in the gas phase[6–9] are complex because there are five peaks in the narrow energy range (11.76–13.96 eV), thus leading to a range of possible assignments for this region. A schematic diagram of this spectrum is shown in Fig. 2. A summary of assignments by elementary MO considerations, together with He(I), He(II) intensity changes, and considerations of photoionization cross sections under synchrotron irradiation[10] support the early uv photoelectron spectral assignments.[6–9]

The x-ray photoelectron spectra of $TiCl_4$ and related molecules show well-defined satellites on the $Ti(^2P_{3/2})$ line at 4.0 and 9.4 eV above the main line.[11] However, interpretation of these shake-up states, in terms of the vuv data, has been controversial[12,13] owing to the intensity ratio of the two bands.

Several theoretical studies have focused upon these spectroscopic results; thus the vuv spectrum has been partially assigned by using both semiempirical methods,[2,5,14–17] SCF-Xα methods[18–20] and small scale CI calculations.[21] However, there are no *ab initio* calculations which include a detailed analysis of electron correlations.

Assignment of the uv photoelectron spectrum by means of theoretical methods, using semiempirical or Xα calculations, is summarized in the study on the Green's function method;[22] this gave the ionization ordering,

$$(1t_1)^{-1} < (3t_2)^{-1} < (1e)^{-1}, \quad (2t_2)^{-1} < (2a_1)^{-1}.$$

This order is the same for the lowest three IPs as that obtained by open-shell INDO-SCF (intermediate neglect of differential overlap) calculations.[23]

In this paper, we reinvestigate the excited and ionized states of $TiCl_4$, in order to put the theoretical aspect on a more rigorous level. We use the SAC (symmetry adapted cluster expansion)[24]/SAC-CI method,[25] which has been applied to a number of molecules including transition metal complexes.[26–28] This method has been shown to be useful for investigating spectroscopies of excited and ionized states of molecules and given many reliable new assignments for the experimental spectra. In addition, a parallel investigation using multireference CI has been performed; we have previously found that this method is capable of giving a good interpretation of the vuv spectra of aromatic compounds.[29,30] The present paper presents the consolidated results of the two approaches.

II. COMPUTATIONAL DETAILS

The structure of $TiCl_4$ is tetrahedral with Ti–Cl bond length of 2.17 Å.[31] Since we did not include structural relaxation effects in the present study, we focus upon vertical excitations of the $TiCl_4$ molecule. In all the calculations [including both the SAC-CI and MRD-CI (multireference double excitation) ones below], the computations were performed in the C_{2V} subset of T_D; under these circumstances the MO identities are

 0021-9606/92/162561-10$006.00

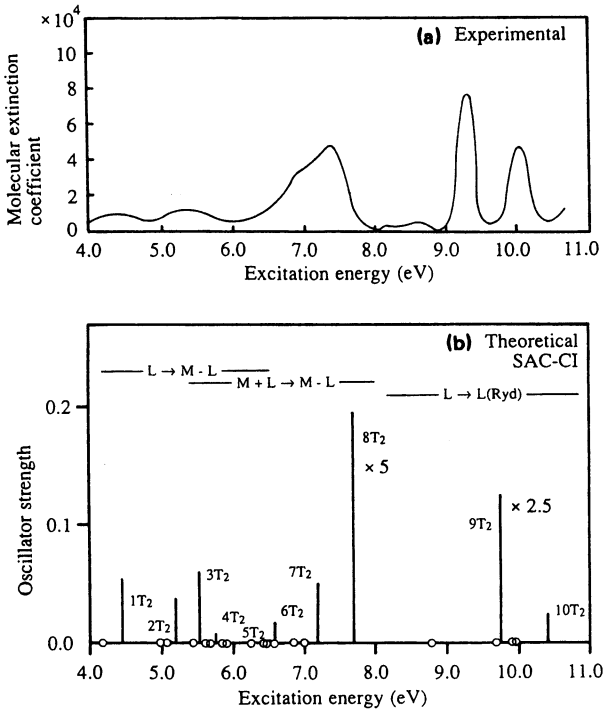

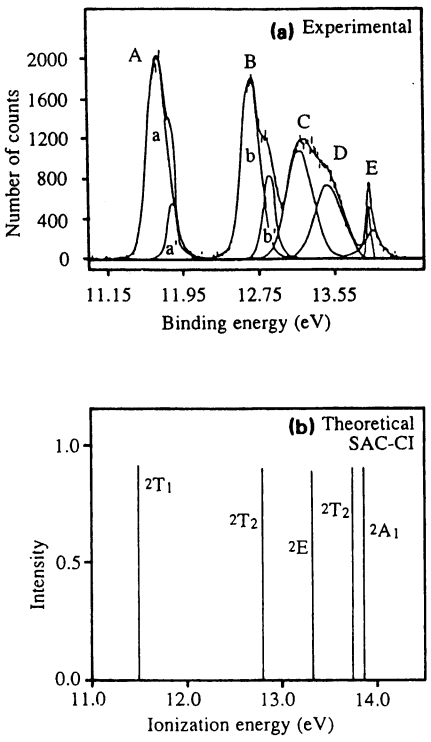

FIG. 1 (a) Experimental (b) SAC-CI theoretical excitation spectra of $TiCl_4$. For the $8T_2$ and $9T_2$ states the intensities given for the SAC-CI spectrum are 1/5 and 2/5 of the calculated ones.

FIG. 2 (a) Experimental spectrum, (b) SAC-CI theoretical outer-valence ionization spectrum, and (c) SAC-CI theoretical inner-valence ionization spectrum for $TiCl_4$. (1): $(1a_1)^{-1}$, (2): $(1t_2)^{-1}$, (3): $(2a_1)^{-1}$, (4): $(2t_2)^{-1}$, (5): $(1e)^{-1}$, (6): $(3t_2)^{-1}$.

$t_1(a_2+b_1+b_2), t_2(a_1+b_1+b_2)$, $e(a_1+a_2)$, and $a_1(a_1)$

with the inverse relationships shown in Table IV below. The B_1 and B_2 states are degenerate under these circumstances; there are no a_2 (T_D) MOs for $TiCl_4$ with the present basis sets. The T_D symmetry of $TiCl_4$ leads to the following open shell direct products of MOs in the low-lying excited states:

$$t_1 \times t_2 = T_1 + T_2 + A_2 + E, \quad t_2 \times t_2 = T_1 + T_2 + A_1 + E,$$

$$t_1 \times e = T_1 + T_2, \quad t_2 \times e = T_1 + T_2, \quad t_2 \times a_2 = T_1,$$

$$t_1 \times a_2 = T_2, \quad e \times e = A_1 + A_2 + E.$$

We tested two types of basis sets in these parallel studies, the effective core potentials of Hay and Wadt[32] and the all-electron GTO (Gaussian-type orbital) basis of Huzinaga,[33] but with various expansions and appended Rydberg functions, as described below.

A. Examination of basis sets

Initially in the SAC-CI study, we calculated the atomic excitation spectra of Ti^{3+}, Cl atom and Cl anion, and determined the final set to best reproduce the excitation energies of $TiCl_4$. Since the $TiCl_4$ bonds are polarized Ti^+–Cl^-, and some of the excitations were expected to approximate to ligand excitations, we examined the effect of diffuse functions on Cl that would produce an anion-type basis. Table I shows the excitation energies of Ti^{3+} and the Cl atom together with the experimental values.[34] There exist large discrepancies between the theoretical results with the ECP (effective core potential) and the experimental values; about 5.5 eV for the $4p$ state of Ti^{3+}. With the all-electron basis set of Huzinaga on the other hand, we can reproduce the experimental values within 0.20 eV. Furthermore, extensive tests of this ECP by both the SAC-CI and MRD-CI procedures failed to produce an acceptable envelope for the vuv excitation spectrum of $TiCl_4$. Table II shows $3p \rightarrow 4s$, $4p$ excitation energies of the Cl anion calculated with and without the anion s, p basis $(\zeta_s = \zeta_p = 0.049)$.[36] The effect is as large as 0.49 eV for some states and important for obtaining the correct ordering of the $4s$ and $4p$ states.

In the initial phase of the MRD-CI calculations, the ECP (Ref. 33) was performed with a Ti $[3s2p3d]$ and Cl $[2s2p]$ valence shell, and an active space of 55 MOs and 24 electrons. Not only was the 8–10 eV region poorly interpreted, but the lowest excitations were also difficult to assign to the experimental envelope. Increase of the valence

TABLE I. Excitation energies of Ti^{3+} ion and Cl atom calculated by the SAC-CI method (in eV).

State	Expt.[a]	Basis set: ECP[b]	Basis set: All electron[c]
Ti^{3+} ion			
$4s$	9.97	10.61	10.18
$4p$	15.86, 15.96	21.44	15.64
$4d$	24.40, 24.41	25.15	24.55
$5s$	26.33	26.91	27.03
$5p$	28.59, 28.63	33.19	28.58
Cl atom[d]			
$(3p\rightarrow 4s)$			
^2P	9.20, 9.28	9.30	9.43
^2D	10.43, 10.43	10.82	10.86
$(3p\rightarrow 4p)$			
^2S	10.56	10.37	10.61
^2P	10.56, 10.65	10.56	10.74
^2P	11.69, 11.71	12.00	12.14
^2F	11.79, 11.80	12.19	12.24

[a]Reference 35.
[b]Basis sets in Ref. 33 are used.
[c]Basis sets in Ref. 34 are used.
[d]SAC-CI (R general) method (Ref. 35) is used.

shell basis to Ti [$3s4p3d1f$] and Cl [$2s2p1d$] and a similar active space led to little improvement. Further, there were technical problems of extrapolation in the MRD-CI calculations owing to coupling of the roots into groups with similar composition, but with wide energy ranges.[37]

In view of the problems with fitting the experimental vuv envelope for $TiCl_4$, we decided to abandon the ECP, and further tests of the all-electron bases were undertaken. We finally selected the following three sets for the molecular calculations. Some features are summarized in Table III.

Set I. This set was designed, based on the calculations shown in Tables I and II, for studying singlet and triplet states by the SAC-CI method. For the Ti atom, Huzinaga's $(14s8p5d)/[6s2p3d]$ set[33] augmented with two p-type functions with $\zeta_p = 0.15, 0.073$ to represent the $4p$ orbitals was utilized. For the Cl atoms, Huzinaga's $(11s8p)/[4s3p]$ set[33] enlarged with Rydberg s, p functions of $\zeta_s = 0.025$, $\zeta_p = 0.02$, and anion s, p functions with the exponents of $\zeta_s = \zeta_p = 0.049$ (Ref. 36) seemed appropriate. As shown in Table II, the anion basis is important for describing $3s\rightarrow 4s$, $4p$ excitations of the Cl anion. Thus the final set for the $TiCl_4$ molecule consisted of 120 functions. For the SAC-CI study the 12 highest occupied orbitals and 46 lowest virtual orbitals were selected for the active space.

TABLE II. Excitation energies of Cl anion with and without the anion basis calculated by the SAC-CI method (in eV).

State	Degeneracy	Anion basis[a]: Without Singlet	Without Triplet	With Singlet	With Triplet	Effect of anion basis
$(3p\rightarrow 4s)$	3	4.62	4.43	4.16	4.08	−0.46
$(3p\rightarrow 4p)$	5	4.55	4.49	4.39	4.36	−0.16
	3	4.61	4.60	4.44	4.43	−0.17
	1	5.02	4.27	4.53	4.22	−0.49

[a]Anion bases with the exponents of $\zeta_s = \zeta_p = 0.049$ are included or not included to the all electron [$4s3p$] set plus Rydberg basis with the exponents of $\zeta_s = 0.025, \zeta_p = 0.020$.

Set II. This set was used for the ionized states (SAC-CI only). The Rydberg functions and the anion basis on the Cl atom were removed from the basis set of Set I. The total number of basis functions was 88. The active space was composed of the 16 highest occupied orbitals and 42 lowest unoccupied orbitals.

In all the SAC-CI calculations, the Hartree–Fock SCF MOs of the ground state were obtained by use of the HONDO7[38] program, and were utilized as the reference set in the subsequent SAC/SAC-CI calculations performed with the SAC85 program.[39]

Set III. The MRD-CI study used an all-electron triple zeta valence set[40(a)] on both Ti and Cl, augmented by Ti [$1s1p$] of Rydberg type (ζ_s 0.0314,ζ_p 0.016)[40(b)] and Cl [$1d$] polarization function. This led to 156 basis functions; the CI subset consisted of 52 MOs and 24 electrons with up to 69 main reference functions (69M20R in the usual[41(a),41(b)] MRD-CI terminology). The diagonalization dimensions were around 13 000 varying with irreducible representation, with a total selected configuration space of 400 000. The SCF calculations preceding the MRD-CI study were performed with the GAMESS suite of programs.[42]

B. Details of the SAC-CI calculation

Electron correlation in the ground state was computed by the SAC theory[24] and those in the excited and ionized states by the SAC-CI theory.[25] We included all single excitations and selected double excitations in the linked terms. The contributions of triple and quadruple excitations are considered in the unlinked terms. To reduce the size of the matrices involved, we performed configuration selection as reported previously.[44] For the singlet and triplet states, the thresholds λ_g and λ_e were set to 2×10^{-5} and 4×10^{-5} a.u., respectively (Set I). Configuration selection was performed for the lowest 20, 17, and 18 SE (single excitation)-CI solutions for the $^1A_1$, $^1A_2$, and $^1B_1$ states, respectively, and lowest 10 solutions for each symmetry of the triplet states. For the ionized states, λ_g and λ_e were set to 3×10^{-5} and 1×10^{-5} a.u. (Set II). The resultant dimensions of the present calculations are shown in Table IV.

III. THE $TiCl_4$ GROUND STATE

The HF configuration of the ground state of $TiCl_4$ and the orbital character in each of the all-electron calculations are shown in Table V. We adopted the valence shell numbering of previous work[22] for easy comparison throughout the present paper. The lowest occupied valence MOs, $1a_1$ and $1t_2$ are composed of the inner valence $3s$ orbitals of the Cl ligands: four $3s$ AOs split into nondegenerate a_1 and threefold degenerate t_2 MOs, whose orbital energies are very close. The next three occupied MOs $2a_1$, $2t_2$, and $1e$

TABLE III. Basis set, active space, and SCF and correlation energies of the ground state for $TiCl_4$.

	Basis set		SCF		Correlated			
	Ti	Cl	Dimension	Energy (a.u.)	Method	Active space (occ×vac)	Energy	Correlation energy
Set I	[6*s*4*p*3*d*]	[4*s*3*p*] +2*s*2*p* (diffuse)	120	−2685.870 48	SAC/SAC-CI	58 MOs (12×46)	−2685.984 34	−0.113 86
Set II	[6*s*4*p*3*d*]	[4*s*3*p*]	88	−2685.862 84	SAC/SAC-CI	58 MOs (16×42)	−2686.065 60	−0.202 76
Set III	[10*s*8*p*3*d*] +1*s*1*p* (Ryd)	[7*s*4*p*] +1*d* (pol)	156	−2686.684 06	MRD-CI	52 MOs (12×40)	−2686.884 29	−0.210 23

are bonding MOs between Ti and Cl atoms. The Ti 4*s* orbital is used in the $2a_1$ MO and the Ti *d* orbital is used in the $2t_2$ and 1*e* MOs. The highest two occupied MOs, $3t_2$ and $1t_1$, are nonbonding lone-pair orbitals localized on the ligands. We note that the orbital energies of the occupied orbitals $2a_1$, $2t_2$, 1*e*, and $3t_2$ are very close to each other. We will see later that this causes the complexity of the main configurations of the valence excitations and the different assignments in the ionization spectrum.

The lowest unoccupied MOs 2*e* and $4t_2$ are antibonding between Ti and Cl: they have negative orbital energy. The next group of unoccupied orbitals are mainly composed of the Rydberg-type 4*s* and 4*p* orbitals of the Cl ligands, but $6t_2$ is of mixed character of Ti 4*p* and Cl 4*p* orbitals. These orbitals shown in Table V were the only group of MOs found to be important for describing the primary nature of the excited states.

The energy for the ground states of $TiCl_4$ is summarized in Table III. The correlation energy is the difference between the SAC or MRD-CI energy and the SCF energy. The SCF energy indicates the quality of the valence basis set: Set III is by far the best among the basis sets used. The correlation energy of the SAC calculation for Set II is larger than that for Set I because the former involves the correlations of the 3*s* electrons of Cl. The MRD-CI correlation energy is larger than the SAC correlation energy of Set I because it involves angular correlations of Cl represented by the polarization functions.

TABLE IV. Dimensions of the SAC/SAC-CI calculations for $TiCl_4$.

State symmetry		
T_d	C_{2v}	Dimension
Basis set I		
Ground $^1A_1$	$^1A_1$	1326
Excited states		
$^1T_2$, ^1E, $^1A_1$	$^1A_1$	6139
$^1T_1$, ^1E, $^1A_2$	$^1A_2$	6645
$^1T_1$, $^1T_2$	$^1B_1$	5927
$^3T_2$, ^3E, $^3A_1$	$^3A_1$	5309
$^3T_1$, ^3E, $^3A_2$	$^3A_2$	5918
$^3T_1$, $^3T_2$	$^3B_1$	5874
Basis set II		
Ground $^1A_1$	$^1A_1$	2780
Ionized states		
$^2T_2$, ^2E, $^2A_1$	$^2A_1$	2083
$^2T_1$, ^2E, $^2A_2$	$^2A_2$	1001
$^2T_1$, $^2T_2$	$^2B_1$	1777

Table VI shows a population analysis for $TiCl_4$ with different basis sets. We see that atomic populations are very subject to basis set. For example, when we take off the Cl anion bases from Set I, the Ti charge changes from −0.2328 to +0.5199: a large change occurs on the Ti *s* and *d* AO populations. A well-known difficulty of the Mulliken population analysis occurs when the basis set includes very diffuse bases. When the bases do not include the anion basis on Cl, the Ti gross charge is positive(+0.5∼+1.0) and Cl is negative(−0.13∼−0.26), though the charge is still very much basis-set dependent. For further examples, basis sets (Ti/Cl) 149 (7*s*6*p*4*d*/7*s*4*p*1*d*), 156 (Basis III) (11*s*9*p*3*d*/7*s*4*p*1*d*), and 178 (11*s*9*p*4*d*/8*s*5*p*1*d*) give charges on Ti of (+)1.437, 1.027, and 0.661, respectively.

The effect of *f* functions ($\zeta_f = 1.550$, and hence of valence character) was insufficient to justify further investigation (the total *f* population was 0.006). Since $TiCl_4$ is somewhat volatile (bp 137 deg, mp −23 deg), a significant amount of covalence must pertain. The ^{35}Cl NQR (nuclear quadrupole) frequency for $TiCl_4$ is very low,[45,46] and this has led to suggestions of considerable π bonding,[46] also supported by comparison of the lone-pair Cl IPs with related compounds.[47]

TABLE V. Orbital energy and orbital nature of $TiCl_4$.

MO	Orbital energy (a.u.)[a]	Orbital nature[b]	
Valence occupied MO			
$(1a_1)^2$	−1.134 53	L(*s*)	:nonbonding
$(1t_2)^6$	−1.117 58	L(*s*)	:nonbonding
$(2a_1)^2$	−0.569 70	M(*s*)–L(*pσ*)	:weakly antibonding
$(2t_2)^6$	−0.558 65	M(*dσ*)+L(*pσ*)	:*σ* bonding
$(1e)^4$	−0.544 28	M(*dπ*)+L(*pπ*)	:*π* bonding
$(3t_2)^6$	−0.529 94	L(*pπ*)	:nonbonding, lone pair
$(1t_1)^6$	−0.480 81	L(*pπ*)	:nonbonding, lone pair
Low-lying unoccupied MO			
(2*e*)	−0.021 70	M(*dπ*)–L(*pπ*)	:*π* antibonding
$(4t_2)$	−0.011 65	M(*d*)–L(*pσ*,*pπ*)	:*σ*, *π* antibonding
$(3a_1)$	0.025 34	L(*s**)	:Rydberg
$(5t_2)$	0.033 77	L(*p**)	:Rydberg
$(6t_2)$	0.055 71	M(*p**)–L(*p**)	:antibonding
(3*e*)	0.058 14	L(*p**)	:Rydberg

[a]Set I result.

[b]M(*i*), L(*j*) denote valence *i*- and *j*-type orbitals on Ti and Cl atoms, respectively, and the asterisk indicates the Rydberg orbitals. Plus and minus signs show bonding and antibonding characters, respectively.

TABLE VI. Mulliken population analysis for the ground state of $TiCl_4$.

	Mulliken population									
	Ti					Cl				
Basis set	*s*	*p*	*d*[a]	Total	Charge	*s*	*p*	*d*	Total	Charge
Set I without Cl anion basis	5.9244	12.8314	2.7243	21.4801	+0.5199	5.9464	11.1836	···	17.1300	−0.1300
Set I (with Cl anion basis)	7.1365	12.9394	2.1569	22.2328	−0.2328	5.8856	11.0562	···	16.9418	+0.0582
Set II	5.7948	12.8309	2.8235	21.4492	+0.5508	5.9486	11.1891	···	17.1377	−0.1377
Set III	6.3782	12.7210	1.8739	20.9731	+1.0269	5.9441	11.2931	0.0196	17.2568	−0.2568
ECP	0.6777	0.5513	1.6684	2.8974	+1.1026	1.9801	5.2956	···	7.2757	−0.2757

[a]Population in dr^2 is also included in *d*-AO.

IV. EXCITED STATES

A. The overall position

The excitation energies, oscillator strengths, and second moments of the singlet excited states are summarized in Table VII, both for SAC-CI and MRD-CI calculations, while the excitation energies of the low-lying triplet states are given in Table VIII for SAC-CI calculations alone. The MRD-CI results are generally similar to the SAC-CI results, with a standard deviation of corresponding states in a linear regression of 0.349 eV. The discrepancy is smaller at the high energy end of the spectrum than the lower end. This makes it possible to consider only one of the two sets of data in the following discussion; we consider the SAC-CI results from this point, except where indicated. The SAC-CI theoretical spectrum and the experimental (gas phase) absorption spectrum[2] are compared in Fig. 1; dipole forbidden transitions are indicated by circles.

We may divide the excitation spectrum into two regions; that from 4 eV (30 000 cm^{-1}) to 8 eV (70 000 cm^{-1}) (Region I) corresponds to valence excitations, while the range from there up to 10.5 eV (90 000 cm^{-1}) (Region II) involves Rydberg excitations. Region I is further characterized by two kinds of excitations; (a) charge transfer excitation from L(p) nonbonding MOs to M(d)–L(p) antibonding MOs, and (b) the transition from M–L bonding MOs to M–L antibonding MOs. These two types of excitations (a,b) are analogous to those of regions A and B in the study of RuO_4 and OsO_4,[28(b)] where they were well separated, though they are not for $TiCl_4$. This difference arises from the separation of the ionized states of $(L)^{-1}$ and $(M+L)^{-1}$; this is large for RuO_4 and OsO_4, whereas $TiCl_4$ has several ionized states in a very narrow energy range (11.76–13.96 eV).[6–9] The M–L bond in $TiCl_4$ is not as strong as that in RuO_4 and OsO_4, since the TiCl bonds are effectively single, whereas the RuO and OsO bonds are partial double bonds.

In outline, as one can see in Table VII, the lower end of Region I has charge transfer character and the higher end has M–L bonding to antibonding transition character; the intermediate region ($3T_1$ to $6T_1$) has "mixed character." In this sense, we cannot divide Region I and need to treat the two types of excitations together as a valence region. Region II is characterized mainly as the excitation from L(p) nonbonding MO on Cl to L(s^*,p^*) Rydberg MO on Cl, i.e., Rydberg excitation within ligands.

B. Assignment of the Region I spectrum

Region I of the absorption spectrum in Fig. 1 shows four prominent bands at 4.43, 5.38, 7.07, and 7.39 eV.[2] The observed bands have no vibrational structure, which indicates that there are considerable dynamic and static Jahn–Teller effects. In T_d symmetry, only the optical transitions to T_2 states are dipole allowed. In this region, a number of dipole forbidden states of T_1, E, A_1, and A_2 symmetry were found as shown in Table VII. Since these states are located close to dipole allowed transitions, they are able to gain intensity through vibronic coupling.

An unresolved absorption band is observed at 4.0 eV on the shoulder of the first band.[2] This shoulder was interpreted as an electronic dipole forbidden transition and assigned to the $1t_1 \rightarrow 3a_1$ transition by CNDO calculations.[2] In our calculations, the dipole forbidden transition to the $1T_1$ state ($1t_1 \rightarrow 2e$) is calculated at 4.19 eV; another possible assignment for this weak shoulder is a transition to a triplet state. We found several low-lying triplet states in the low energy region, with ten triplet states calculated below 5.50 eV (Table VIII); thus there are two candidates for this shoulder, the $1\,^3T_2(1t_1 \rightarrow 2e)$ and $1\,^3T_1(1t_1 \rightarrow 2e)$ states which are calculated to lie at 4.12 and 4.19 eV, respectively. In conclusion, we cannot specify the origin of this weak shoulder; either, it is a $1T_1$ state which borrows its intensity from the transition to the $1T_2$ state, or it is a spin-forbidden triplet state, that is $1\,^3T_2$ and $1\,^3T_1$. Further spectroscopic measurements in this region are warranted.

The first main band has its maximum at 4.43 eV; this is attributed to the $1T_2$ state ($1t_1 \rightarrow 2e$), calculated at 4.42 eV, and is a transition from chlorine lone-pair MO to the Ti($d\pi$)–Cl($p\pi$) antibonding MO, i.e., a charge transfer transition from the ligand to the metal. The second observed band has its maximum at 5.38 eV. Three dipole allowed transitions are calculated in this energy region; they are the $2T_2$ state ($1t_1 \rightarrow 4t_2$) at 5.22 eV, the $3T_2$ state ($3t_2 \rightarrow 2e$) at 5.53 eV, and the $4T_2$ state ($2t_2 \rightarrow 4t_2$) at 5.74 eV. These three states are assigned to the second band. The $2T_2$ and $3T_2$ states are charge transfer excitation in type, while the $4T_2$ state is the transition from the Ti–Cl bonding to the Ti–Cl antibonding MOs. Consequently, this band has "mixed character" as described above. The intensities of the first two transitions are stronger than that of the third one as seen from Fig. 1.

The band centered at about 7.4 eV has a low energy

TABLE VII. Excitation energies, oscillator strengths, and second moments of singlet excited states for $TiCl_4$

State	Main configurations[a]	SAC-CI Excitation energy	SAC-CI Oscillator strength	SAC-CI Second moment	Expt. BBT[b]	Expt. IR[c]	MRD-CI Excitation energy	MRD-CI Oscillator strength
Ground state		0.0	...	433			0.0	...
Region I								
$1T_1$	$0.89(1t_1\rightarrow 2e)$	4.19	forbidden	433	(4.00)		4.97	0.0
$1T_2$	$0.85(1t_1\rightarrow 2e)$	4.42	5.60×10^{-2}	433	4.43	4.41	5.08	5.10×10^{-2}
$1E$	$0.85(1t_1\rightarrow 4t_2)$	4.99	forbidden	433			6.24	0.0
$2T_1$	$0.67(1t_1\rightarrow 4t_2), 0.23(3t_2\rightarrow 2e)$	4.98	forbidden	434			6.02	0.0
$1A_2$	$0.78(1t_1\rightarrow 4t_2), 0.14(1e\rightarrow 2e)$	5.05	forbidden	433			5.47	0.0
$2T_2$	$0.83(1t_1\rightarrow 4t_2)$	5.22	3.72×10^{-2}	433	5.38	5.31	6.69	4.10×10^{-2}
$3T_1$	$0.48(2t_2\rightarrow 2e), 0.26(3t_2\rightarrow 2e), 0.13(1t_1\rightarrow 4t_2)$	5.44	forbidden	434			6.32	0.0
$3T_2$	$0.80(3t_2\rightarrow 2e)$	5.53	5.97×10^{-2}	433	5.38	5.31	6.93	4.20×10^{-2}
$4T_1$	$0.40(3t_2\rightarrow 2e), 0.37(2t_2\rightarrow 2e)$	5.61	forbidden	434			5.94	0.0
$2E$	$0.70(1e\rightarrow 2e), 0.09(3t_2\rightarrow 4t_2)$	5.70	forbidden	433			6.89	0.0
$4T_2$	$0.83(2t_2\rightarrow 2e)$	5.74	7.63×10^{-3}	433	5.38	5.31	6.95	7.40×10^{-3}
$2A_2$	$0.77(1e\rightarrow 2e), 0.14(1t_1\rightarrow 4t_2)$	5.83	forbidden	433			6.61	0.0
$1A_1$	$0.63(1e\rightarrow 2e), 0.28(2t_2\rightarrow 4t_2)$	5.92	forbidden	433			7.14	0.0
$5T_1$	$0.77(3t_2\rightarrow 4t_2), 0.10(1e\rightarrow 4t_2)$	6.26	forbidden	434			7.07	0.0
$3E$	$0.81(2a_1\rightarrow 2e), 0.06(2t_2\rightarrow 4t_2)$	6.27	forbidden	434			7.22	0.0
$4E$	$0.77(3t_2\rightarrow 4t_2), 0.12(1e\rightarrow 2e)$	6.40	forbidden	433			6.94	0.0
$2A_1$	$0.79(3t_2\rightarrow 4t_2)$	6.45	forbidden	433			7.99	0.0
$5T_2$	$0.61(3t_2\rightarrow 4t_2), 0.14(2t_2\rightarrow 4t_2), 0.11(1e\rightarrow 4t_2)$	6.52	6.14×10^{-4}	433			7.76	3.40×10^{-3}
$6T_1$	$0.77(1e\rightarrow 4t_2), 0.11(3t_2\rightarrow 4t_2)$	6.60	forbidden	434			7.54	0.0
$6T_2$	$0.55(1e\rightarrow 4t_2), 0.22(3t_2\rightarrow 4t_2), 0.10(2t_2\rightarrow 4t_2)$	6.61	1.73×10^{-2}	433			7.85	4.00×10^{-4}
$7T_1$	$0.83(2t_2\rightarrow 4t_2), 0.05(2t_2\rightarrow 2e)$	6.84	forbidden	433			7.99	0.0
$5E$	$0.81(2t_2\rightarrow 4t_2), 0.09(2a_1\rightarrow 2e)$	7.00	forbidden	434			8.07	0.0
$7T_2$	$0.38(2t_2\rightarrow 4t_2), 0.34(2a_1\rightarrow 4t_2), 0.14(1e\rightarrow 4t_2)$	7.20	4.86×10^{-2}	433	7.07	6.85	8.18	1.70×10^{-1}
$3A_1$		...	...	...			8.52	0.0
$8T_2$	$0.52(2a_1\rightarrow 4t_2), 0.15(2t_2\rightarrow 4t_2), 0.09(1e\rightarrow 4t_2)$	7.72	0.982	433	7.39	7.33	8.79	0.591
Region II								
$8T_1$	$0.65(1t_1\rightarrow 3a_1), 0.19(1t_1\rightarrow 4a_1)$	8.81	forbidden	448	(8.18, 8.68)	(8.39, 8.89)	8.67	0.0
$6E$	$0.70(1t_1\rightarrow 5t_2), 0.08(1e\rightarrow 3a_1), 0.05(1t_1\rightarrow 7t_2)$	9.75	forbidden	456			9.71	0.0
$9T_2$	$0.62(1t_1\rightarrow 5t_2), 0.17(3t_2\rightarrow 3a_1)$	9.79	2.86×10^{-1}	453	9.35	9.29	9.84	0.276
$9T_1$	$0.68(1t_1\rightarrow 5t_2), 0.18(1t_1\rightarrow 6t_2)$	9.92	forbidden	456			10.04	0.0
$3A_2$	$0.71(1t_1\rightarrow 5t_2), 0.14(1t_1\rightarrow 6t_2)$	9.95	forbidden	455			9.89	0.0
$10T_2$	$0.25(1t_1\rightarrow 3e), 0.24(1t_1\rightarrow 6t_2), 0.23(3t_2\rightarrow 3a_1), 0.08(1t_1\rightarrow 5t_2)$	10.43	2.39×10^{-2}	455	10.04	9.99	10.23	7.10×10^{-2}

[a]Configurations and square values of the coefficients are listed for those whose square values are larger than 0.04 (SAC-CI results).
[b]Reference 2.
[c]Reference 4.

shoulder at 7.07 eV; the latter is assigned to the $7T_2$ state calculated at 7.20 eV. This state consists of a linear combination of three main configurations; they are $2t_2 \rightarrow 4t_2$, $2a_1 \rightarrow 4t_2$, and $1e \rightarrow 4t_2$; thus configuration interaction is very important for the precise description of this state. Two other dipole allowed transitions are calculated in the 6.5–6.7 eV region, namely, the $5T_2$ state which has a small oscillator strength, and the $6T_2$ state which has a more considerable one. These are attributed to the tail in the lower energy region of the peak at 7.07 eV. Since these transitions are from the Ti–Cl bonding MO to the antibonding MO, the geometries of the excited states would be very much relaxed.

The strong maximum band at 7.39 eV is attributed to the $8T_2$ state, which also has the same excitation nature as both the $7T_2$ and $6T_2$ states. The experimental spectrum shows a very large molecular extinction coefficient for this band; this is in agreement with the SAC-CI and MRD-CI calculations, where we calculate a very intense band (F 0.982). A broad nature of the peak may be attributed to the geometrical relaxation on the excited state.

Robin assigned these two peaks (7.07, 7.39 eV) to

TABLE VIII. SAC-CI excitation energies for the low-lying triplet states of $TiCl_4$.

State	Main configurations[a]	Excitation energy	Expt.[b]
$1\,^3T_2$	$0.85(1t_1\rightarrow 2e)$	4.12	(4.00)
$1\,^3T_1$	$0.88(1t_1\rightarrow 2e)$	4.19	4.43
$2\,^3T_2$	$0.64(1t_1\rightarrow 4t_2),0.23(3t_2\rightarrow 2e)$	4.95	
$1\,^3E$	$0.80(1t_1\rightarrow 4t_2),0.10(1e\rightarrow 2e)$	4.95	
$2\,^3T_1$	$0.60(1t_1\rightarrow 4t_2),0.28(3t_2\rightarrow 2e)$	4.96	
$1\,^3A_1$	$0.72(1e\rightarrow 2e),0.05(3t_2\rightarrow 4t_2)$	5.12	
$1\,^3A_2$	$0.76(1t_2\rightarrow 4t_2),0.16(1e\rightarrow 2e)$	5.12	
$3\,^3T_2$	$0.57(3t_2\rightarrow 2e),0.22(1t_1\rightarrow 4t_2),0.07(1e\rightarrow 4t_2)$	5.32	
$3\,^3T_1$	$0.72(2t_2\rightarrow 2e),0.05(3t_2\rightarrow 2e),0.04(1t_1\rightarrow 4t_2)$	5.36	5.38
$4\,^3T_2$	$0.82(2t_2\rightarrow 2e)$	5.48	

[a]Configurations and square values of the coefficients are listed for those whose square values are larger than 0.04 (SAC-CI results).
[b]Reference 2.

Jahn–Teller distortion originating from the same electronic transition; he suggested the assignment $2t_2 \rightarrow 4t_2$ ($7T_2$). However, he overlooked a possibility of a large oscillator strength of the $2a_1 \rightarrow 4t_2$ transition ($8T_2$ state). Actually, this transition has the largest oscillator strength as shown in Table VII. Therefore, we assign these two peaks to the different electronic transitions; transitions to $7T_2$ and $8T_2$ states.

The previous theoretical studies on the excitation spectrum of $TiCl_4$ either relied upon one-electron energy differences[2,14,15] or were small scale CI calculations, in which only 192 singly excited configurations were considered;[21] the latter also concentrated upon the T_2 states with the exception of the lowest T_1 state. These early CI calculations inevitably gave considerable errors in excitation energy relative to experiment (often 2–3 eV), but the general order of upper and lower states follows the present work. The SCF-Xα transition state calculations of Tossell[12(a)] show a number of similarities to the present work, but comparison is not immediately obvious, since the overall state symmetries were not given. The $1e$ to $2e$ and $4t_2$ states are calculated low by about 2 eV in that study and he assigned the shoulder of the third band to the transition $1e\rightarrow 2e$. However, this excitation is dipole forbidden. Another SCF-Xα calculation also gave slightly different assignments.[18] The difference between our results and these SCF-Xα results seems to exist in the ordering of the $2a_1$ and $2t_2$ orbitals.

The shake-up states observed in the x-ray photoelectron spectrum agree for the 4.0 eV excitation accompanying the $2p$ ionization as $1T_2$, $1t_1$ to $2e$.[13] The higher excitations computed by Veal *et al.*[13] at 5.0 and 10.4 eV do not correspond closely to the present results for the same processes; the present results suggest that $2a_1$ to $4t_2$ excitation is more likely at 7.4 eV; with further excitations L to L* above 9 eV, as discussed below.

C. Region II spectral assignments

We see from Table VII that the electronic component of the second moments of the states in Region I lie in the range 433–434 a.u., essentially the same as the ground state value of 433 a.u. This is another reason why the excited states in Region I are assigned as valence states. On the other hand, most of the states in Region II have larger second moments of about 455 a.u. suggesting a Rydberg set of transitions.

The dipole forbidden transition to the $8T_1$ state is calculated at 8.81 eV and its second moment is estimated 448 a.u. This transition may correspond to the weak absorption band at 8.68 eV in the experimental spectrum. We were unable to compute a singlet excited T_2 state which is assignable to the weak absorption at 8.18 eV. This weak absorption may also be due to a triplet state.

The strong two peaks observed at 9.35 and 10.04 eV are assigned to the $9T_2$ and the $10T_2$ states calculated at 9.79 and 10.43 eV, respectively. Previous workers have offered alternative assignments; thus Tossell assigned these bands to the transition from Cl($3p$) to the Ti($4s$,$4p$)–Cl($3p$) antibonding MO by SCF-Xα-SW calculations,[12(a)] while Robin suggested the assignment to the Rydberg excitation within the Cl atoms ($3p\rightarrow 4p$) from the similarity of the term values to that transition in the CCl_4 and related molecules.[5] Thus he concluded that the first peak at 9.35 eV originates from the $1t_1$ MO and the second peak at 10.04 eV is from the $3t_2$ MO.

Our result supports Robin's assignment.[5] The first peak is calculated at 9.79 eV and its main configuration is $1t_1 \rightarrow 5t_2$: the transition from the Cl lone-pair $3p$ orbital to the Rydberg $4p$ orbital of Cl. We see a small admixture of the $3t_2 \rightarrow 3a_1$ transition which is a $3p\rightarrow 4s$ Rydberg transition within chlorine. The $10T_2$ state is also a pure Rydberg excitation within the Cl ligands and is described by the linear combination of the excitations $1t_1 \rightarrow 3e$, $1t_1 \rightarrow 6t_2$, and $3t_2 \rightarrow 3a_1$. A difference from the $9T_2$ state is a mixing of the outer p orbital of the Ti atom in the $6t_2$ orbital. Thus the orbital basis must contain Rydberg-type and anion bases for description of these states quantitatively.

In conclusion, the SAC-CI and MRD-CI calculations give essentially consistent assignments of the spectrum, supporting the validity of the present assignments. The average discrepancy between theoretical and experimental values for the excitation spectrum is 0.22 eV for the SAC-CI case.

V. IONIZED STATES AND ASSIGNMENT OF THE PHOTOELECTRON SPECTRUM

Ionization potentials and intensities for $TiCl_4$ calculated by the SAC-CI method are compared with experimental values and the results of the Green's function approach in Table IX. Theoretical and experimental ionization spectra for the outer valence region are shown in Fig. 2. For the inner valence region, only the theoretical spectrum is shown, since no experimental data have been reported. Theoretical intensities are calculated with the use of the monopole approximation.[49]

As noted in the introduction, differing assignments for the outer valence region[7] have been proposed, although there is common agreement over the identity of the first peaks;[22] if we use the notation of Egdell *et al.*,[7] the first two bands A and B are assigned to $(1t_1)^{-1}$ and $(3t_2)^{-1}$, respec-

TABLE IX. Ionization potentials of $TiCl_4$.

State			Expt. LSW[a]	Expt. BPT[b]	Koopmans	SAC-CI IP (Δ[c])	SAC-CI Intensity[d]	2*ph*-TDA[e]
Outer valence ionization[f]								
A	$1\,^2T_1$	$(1t_1)^{-1}$	11.80	11.69	13.09	11.38(−0.42)	0.88	11.70
B	$1\,^2T_2$	$(3t_2)^{-1}$	12.79	12.67	14.44	12.69(−0.10)	0.88	12.98
C	$1\,^2E$	$(1e)^{-1}$	13.29	13.17	14.83	13.25(−0.04)	0.87	13.44
D	$2\,^2T_2$	$(2t_2)^{-1}$	13.54	13.46	15.21	13.52(−0.02)	0.86	13.69
E	$1\,^2A_1$	$(2a_1)^{-1}$	13.98	13.91	15.49	13.61(−0.37)	0.87	13.91
Inner valence ionization[g]								
	^2E					18.14[h]	...	
	$^2A_1$					18.20[h]	...	
	$^2T_2$					18.24[h]	...	
	$^2T_2$	0.007(2)[i]			30.43	25.19	0.010	
		0.025(6)				25.35	0.029	
		0.013(2)				25.78	0.017	
		0.117(2), 0.033(4)				25.96	0.150	
		0.009(2)				26.52	0.018	
		0.024(4), 0.009(2)				26.63	0.035	
		0.018(6)				26.87	0.018	
		0.283(2)				27.25	0.284	
		0.005(2)				27.29	0.005	
		0.184(2)				27.52	0.184	
		0.026(2)				27.77	0.026	
		0.021(2)				27.87	0.022	
		0.029(2)				28.27	0.030	
		0.043(2)				29.00	0.044	
		0.064(2)				29.08	0.064	
	$^2A_1$	0.101(1), 0.012(3)			30.90	26.20	0.113	
		0.048(3)				26.86	0.049	
		0.104(1)				27.37	0.104	
		0.341(1)				27.78	0.342	
		0.010(1)				27.83	0.010	
		0.038(1)				28.30	0.039	
		0.037(1)				28.61	0.038	
		0.026(1)				29.08	0.027	
		0.141(1)				29.15	0.142	
		0.008(1)				29.34	0.008	
	^2E	0.009(5)				25.37	0.009	
		0.018(5)				25.93	0.018	
		0.021(5)				26.22	0.020	
		0.011(5)				26.79	0.011	

[a]Reference 10.
[b]Reference 9.
[c]Deviation from experimental value.
[d]Only the states whose intensity is larger than 0.005 are tabulated.
[e]Reference 22.
[f]Figure 2(b).
[g]Figure 2(c).
[h]Many satellite peaks with very small monopole intensities (<0.001) are calculated in the energy region 18–25 eV. We give only the first three peaks in the table.
[i]Contribution of one-electron process. (1): $(1a_1)^{-1}$, (2): $(1t_2)^{-1}$, (3): $(2a_1)^{-1}$, (4): $(2t_2)^{-1}$, (5): $(1e)^{-1}$, (6): $(3t_2)^{-1}$.

tively. Bancroft *et al.* measured He I and He II photoelectron spectra[9] and proposed the ordering $(1e)^{-1} < (2a_1)^{-1} < (2t_2)^{-1}$ for the bands *C*, *D*, and *E* from the proportion of *d* character in each orbital. A recent MS Xα study also gave the same ordering.[50] On the other hand, analysis by synchrotron radiation[10] and theoretical investigation by the Green's function method[22] gives the order $(1e)^{-1} < (2t_2)^{-1} < (2a_1)^{-1}$. The present results support the latter assignment. Overlapping bands $(C+D)$ correspond to $[(1e)^{-1} + (2t_2)^{-1}]$, which are calculated at 13.25 and 13.52 eV; band *E* is attributed to $(2a_1)^{-1}$. These five states are located in the low energy region and away from shake up states. Therefore, monopole intensities for these states are relatively large. The average discrepancies between theory and experimental values for the outer valence ionization is 0.19 eV.

Next we examine the fine structures in the bands *A* and *B*. There exist weak shoulders in these bands and the splitting between the main peak and the shoulder is observed as 0.145 eV for band *A* and 0.196 eV for band *B*. Bancroft *et al.* estimated[9] the vibrational broadening only for the a_1 mode and gave the vibrational progressions for each band. We estimated the spin-orbit effect for the $(1t_1)^{-1}$ state in the way reported previously[51] and obtained the splitting as 0.058 eV, which is only one third of the observed splitting. The vibrational frequencies[52] of the nomal modes were also not enough to explain the experimental splitting ($\nu_1=0.0482$, $\nu_2=0.0141$, $\nu_3=0.0617$, and $\nu_4=0.0169$ eV). Therefore, we attribute these shoulders to the combination of the spin-orbit interaction, vibronic coupling, and Jahn–Teller effect, as Bancroft *et al.* considered.[9]

Lastly, we investigate the inner valence region; a large number of shake-up states were calculated with onset at 18.3 eV. They are largely separated from the Koopmans'-type ionization (one-electron) processes. Furthermore, the satellite peaks in the low energy region are calculated to have very weak intensities (less than 0.001). Therefore, we show in Fig. 2(c) the calculated satellite peaks in the region greater than 25 eV. Ionizations from $1a_1$ and $1t_2$ show a breakdown of the Koopmans' picture. Shake-up states with symmetry $^2T_2$ and $^2A_1$ mix with these one-electron processes in the range 25.0–30.0 eV. They have considerable intensity through final state correlation. These features were also obtained by the Green's function approach.[22] It was reported that the halogen 3*s* subshells have a low cross section under uv excitation,[8] so there is no experimental information for this energy region.

VI. CONCLUSION

We have applied the SAC-CI and the MRD-CI methods to the calculation of the excited and ionized states of $TiCl_4$. We have successfully reproduced the whole energy region of the experimental spectra. We give several new assignments and a detailed picture for the excitation spectrum of $TiCl_4$. The spectrum is divided into two regions; Region I, 4–8 eV and Region II 8–10.5 eV. Region I involves valence excitations and Region II Rydberg excitations within Cl ligands. Since the occupied valence MOs lie in a narrow energy range, the excitation nature in Region I is very complex for this molecule, and there are considerable configuration mixings in the states. In Region I, the lower excitations are from the Cl lone-pair MO to the (metal *d*–ligand *p*) antibonding MO and thus they are electron transfer excitations from ligand to metal. The higher excitations in Region I are from M–L bonding MO to M–L antibonding MO, so that large geometrical relaxation is expected after the transitions. The excitations in the medium energy range (around 6.5 eV) are therefore mixtures of both types of excitations. In addition to the dipole-allowed transitions, a large number of dipole-forbidden states were calculated. It was also found that many triplet states exist in the low energy region. These states may be responsible for weak features in the vuv spectrum. The strong peaks observed at 9.35 and 10.04 eV of Region II are assigned to Rydberg-type excitations, $3p\rightarrow 4p$ within the Cl ligands in accordance with the earlier Robin's assignment. For the peak at 9.35 eV, a small admixture of the Cl $3p\rightarrow 4s$ Rydberg transition is found and for the peak at 10.04 eV, a mixing of the titanium outer $4p$ orbital is calculated.

For the ionized spectrum, our present calculations confirm the assignments of Egdell and Orchard[8] from experimental observations, and the theoretical study of von Niessen.[22] The ordering of the ionized states in the outer valence region is calculated as $(1t_1)^{-1}<(3t_2)^{-1}<(1e)^{-1}<(2t_2)^{-1}<(2a_1)^{-1}$. Many shake-up states were calculated in the inner valence region. Though these two-electron processes start from 18.3 eV, the observable states whose intensities are larger than 0.005 only appear above 25.0 eV. Further experimental study of this region is required.

ACKNOWLEDGMENTS

The SAC-CI calculations were performed on the FACOM M780 computer at the Data Processing Center of Kyoto University and the HITAC M-680H and S-820 computer at the Institute for Molecular Science. The MRD-CI study was performed on the Rutherford–Appleton Laboratory Cray XMP-48. This study has been supported by a Grant-in-Aid for Scientific Research from the Japanese Ministry of Education, Science and Culture; by the Kurata Foundation; and by the U.K. Science and Engineering Research Council. The authors wish to thank British Council, Japan Society for the Promotion of Science, and the Royal Society for supporting scholar exchange programs for promoting this collaboration.

[1] D. S. Alderdice, J. Mol. Spectrosc. **15**, 509 (1965).
[2] C. A. Becker, C. J. Ballhausen, and I. Trabjerg, Theor. Chim. Acta **13**, 355 (1969).
[3] C. Dijkgraaf and J. P. G. Rousseau, Spectrochim. Acta A **25**, 1831 (1969).
[4] A. A. Iverson and B. R. Russell, Spectrochim. Acta A **29**, 715 (1973).
[5] M. B. Robin, *Higher Excited States of Polyatomic Molecules* (Academic, New York, 1975), Vol. 3, p. 383.
[6] J. C. Green, M. L. H. Green, P. J. Joachim, A. F. Orchard, and D. W. Turner, Philos. Trans. R. Soc. London, Ser. A **268**, 111 (1970).
[7] R. G. Egdell, A. F. Orchard, D. R. Lloyd, and N. V. Richardson, J. Electron Spectrosc. Relat. Phenom. **12**, 415 (1977).
[8] R. G. Egdell and A. F. Orchard, J. Chem. Soc. Faraday Trans. 2 **74**, 485 (1978).
[9] G. M. Bancroft, E. Pellach, and J. S. Tse, Inorg. Chem. **21**, 2950 (1982).
[10] M. Lubcke, B. F. Sonntag, and H. E. Wetel, *Conference Proceedings, International Conference on X-ray and Inner-Shell Processes in Atoms, Molecules, and Solids*, edited by A. Meisel (Karl-Marx-Universitat, Leipzig, 1984), Abstracts Part I, p. 281.
[11] B. Wallbank, J. S. H. Q. Perera, D. C. Frost, and C. A. McDowell, J. Chem. Phys. **69**, 5405 (1978).
[12] (a) J. A. Tossell, Chem. Phys. Lett. **65**, 371 (1979); (b) A. Gupta and J. A. Tossell, J. Electron Spectrosc. Relat. Phenom. **26**, 223 (1982); (c) J. S. Tse, Chem. Phys. Lett. **373**, 15 (1981).
[13] B. W. Veal, K. Lee, and D. E. Ellis, Phys. Rev. A **37**, 1839 (1988).
[14] C. A. L. Becker and J. P. Dahl, Theor. Chim. Acta **14**, 26 (1969).
[15] T. Parameswaran and D. E. Ellis, J. Chem. Phys. **58**, 2088 (1973).
[16] S. S. L. Surana and A. Muller, Chem. Phys. Lett. **67**, 527 (1979).
[17] A. Golebiewski and M. Witko, Acta Phys. Pol. A **51**, 629 (1977).
[18] A. E. Foti, V. H. Smith, Jr., and M. A. Whitehead, Mol. Phys. **45**, 385 (1982).
[19] A. Golebiewski and M. Witko, Acta Phys. Pol. A **57**, 585 (1980).

[20] S. A. Titov, Teor. Eksp. Khim. **20**, 709 (1984).
[21] I. H. Hillier and J. Kendrick, Inorg. Chem. **15**, 520 (1976).
[22] W. von Niessen, Inorg. Chem. **26**, 567 (1987).
[23] D. R. Traux, J. A. Geer, and T. Ziegler, J. Chem. Phys. **59**, 6662 (1973).
[24] H. Nakatsuji and K. Hirao, J. Chem. Phys. **68**, 2053 (1978).
[25] H. Nakatsuji, Chem. Phys. Lett. **59**, 362 (1978); **67**, 329, 334 (1979).
[26] H. Nakatsuji, Acta Chim. Acad. Sci. Hung. (in press).
[27] (a) H. Nakatsuji, J. Chem. Phys. **80**, 3703 (1984); (b) H. Nakatsuji, O. Kitao, and T. Yonezawa, *ibid.* **83**, 723 (1985); (c) H. Nakatsuji and O. Kitao, *ibid.* **87**, 1169 (1987); (d) O. Kitao and H. Nakatsuji, Chem. Phys. Lett. **143**, 528 (1988).
[28] (a) H. Nakatsuji and S. Saito, J. Chem. Phys. **93**, 1865 (1990); (b) H. Nakatsuji and S. Saito, Int. J. Quantum Chem. **39**, 93 (1991); (c) H. Nakatsuji, M. Sugimoto, and S. Saito, Inorg. Chem. **29**, 3095 (1990).
[29] M. H. Palmer, I. C. Walker, M. F. Guest, and A. Hopkirk, Chem. Phys. **147**, 19 (1990).
[30] I. C. Walker and M. H. Palmer, Chem. Phys. **153**, 169 (1991).
[31] Y. Morino and U. Uehara, J. Chem. Phys. **45**, 4543 (1966).
[32] P. J. Hay and W. R. Wadt, J. Chem. Phys. **82**, 299 (1985).
[33] S. Huzinaga, J. Andzelm, M. Klobukowski, E. Radzio-Andzelm, Y. Sakai, and H. Tatewaki, *Gaussian Basis Sets for Molecular Calculations* (Elsevier, Amsterdam, 1984).
[34] C. E. Moore, U. S. Natl. Bur. Stand. Circ. No 467, Vol. I (1949).
[35] H. Nakatsuji, Chem. Phys. Lett. **177**, 331 (1991).
[36] T. H. Dunning, Jr. and P. J. Hay, in *Methods of Electronic Structure Theory*, edited by H. F. Schaefer III (Plenum, New York, 1977).
[37] It was clear that one of the problems of MRD-CI was coupling of roots, often in groups of four, and that these were well separated in energy; extrapolation based upon only some members of the group led to perturbed energies, relative to those obtained when all members of the group were present. Hence it became imperative to expand the number of roots simultaneously determined in MRD-CI from 10 to 20. This caused extensive modification of the code, with major array expansions. A further problem with the MRD-CI method here, is the balancing of the reference set to obtain accurately degenerate roots for E and T states. In general, even with up to 70 main reference functions, it was not possible to obtain degenerate roots closer than about 0.1 eV, although this was sometimes reduced to 0.02 eV; the problem arises from the differing numbers of a_1 and a_2 MOs from b_1 and b_2, and is thus not capable of being exactly solved. In general this did not lead to problems of assignment; the result from the larger diagonalization is quoted in these circumstances. However, there are no such problems in SAC-CI and the degeneracy was kept to within 0.02 eV.
[38] M. Dupuis, J. D. Watts, H. O. Viller, and G. J. B. Hurst, Program System HONDO7, Program Library No. 544, Computer Center of the Institute for Molecular Science (1989).
[39] H. Nakatsuji, Program system for the SAC and SAC-CI calculations for ground, excited, ionized and electron-attached states of molecules, Program Library No. 146 (Y4/SAC), Data Processing Center of Kyoto University, 1985; H. Nakatsuji, Program Library SAC85 (No. 1396), Computer Center of the Institute for Molecular Science, Okazaki, 1986.
[40] (a) A. J. H. Watchers, J. Chem. Phys. **52**, 1033 (1970); (b) D. M. Hood, R. M. Pitzer, and H. F. Schaefer III, *ibid.* **71**, 705 (1979).
[41] (a) R. J. Buenker, in *Proc. of the Workshop on Quantum Chemistry and Molecular Physics, Wollongong, Australia, 1980*, edited by P. G. Burton (Wollongong University, Wollongong, 1980); (b) R. J. Buenker and R. A. Phillips, J. Mol. Struct. (THEOCHEM) **123**, 291 (1985).
[42] M. Dupuis, D. Spangler, and J. J. Wendoloski, NRCC Software Catalog, Vol. 1, GAMESS, Program QC01 (1980); M. F. Guest and P. Sherwood, GAMESS User's Guide and Reference Manual (SERC Daresbury Laboratory, 1991).
[43] H. Nakatsuji, Theor. Chem. Acta. **71**, 201 (1987).
[44] H. Nakatsuji, Chem. Phys. **75**, 425 (1983).
[45] H. G. Dehmelt, J. Chem. Phys. **21**, 380 (1953).
[46] R. P. Hamlen and W. S. Koski, J. Chem. Phys. **25**, 360 (1956).
[47] E. A. C. Lucken, *Nuclear Quadrupole Coupling Constants* (Academic, London, 1969), Chap. 13, p. 308.
[48] W. L. Jolly, Chem. Phys. Lett. **100**, 546 (1983).
[49] R. L. Martin and D. A. Shirley, J. Chem. Phys. **64**, 3685 (1976).
[50] V. Subramanian, M. Vijayakumar, and T. Ramasami, Chem. Phys. Lett. **182**, 232 (1991).
[51] (a) H. Nakatsuji, Y. Matsuzaki, and T. Yonezawa, J. Chem. Phys. **88**, 5759 (1988); (b) C. A. Masmanidis, H. H. Jaffe, and R. L. Ellis, J. Phys. Chem. **79**, 2052 (1975); (c) S. Kato, R. L. Jaffe, A. Komornicki, and K. Morokuma, J. Chem. Phys. **78**, 4567 (1983).
[52] T. Shimanouchi, J. Phys. Chem. Ref. Data **6**, 993 (1977).